Chapter 6

Shadowing Corrections to the Singlet Structure Function and Behaviour of F_2 Slope

6.1 Introduction

Perturbative QCD manifests that the sea quark distributions, in a hadron evolves rapidly with $\ln(1/x)$ at fixed Q^2 in the same manner as the gluon distribution $xg(x, Q^2)$. However in the region of very small-x the sharp growth of the sea quark density is expected to slow down eventually in order to restore the Froissart bound [1, 2] on physical cross sections. In general the gluon recombination processes, which lead to the nonlinear or shadowing corrections to the linear QCD evolution, is considered to be responsible for this taming behaviour. The sea quark distribution, which overshadows the valence quarks at small x, is supposed to be generated through gluons and therefore it is extensively believed that the gluon and sea quark distribution functions almost feel the same effect of shadowing. The nonlinear or shadowing corrections in DIS arise due to two processes, one is the taming of the gluon density as a result of gluon recombination $gg \to g$ and the other is the Glauber-like rescattering of the $q\bar{q}$ fluctuations off gluons [3]. The second process can also be regarded as a parton recombination, particularly as a recombination of gluons into a quark-antiquark pair, $gg \to q\bar{q}$. Gribov, Levin and Ryskin (GLR-MQ) [4], at the onset, investigated the shadowing corrections of gluon recombination to the parton distributions i.e quark and gluon distribution. Following that Mueller and Qiu (MQ) [3, 5] completed the

equation numerically using a perturbative calculation of the recombination probabilities in the DLLA, and also formulated the equation for the conversion of gluons to sea quarks. This is a triumph of great significance as it empowers the GLR-MQ equation to be applied phenomenologically and thus provides the connection to experiments. This equation was made widely applicable in order to include the contributions from more higher order corrections in the Glauber-Mueller formula [3].

In this chapter, we solve the GLR-MQ equation for sea quark distribution incorporating the well known Regge like ansatz and investigate the effect of shadowing corrections on the small-x and moderate-Q^2 behaviour of singlet structure function. Our predictions of x and Q^2 dependence of singlet structure function with shadowing corrections are compared with NMC [6] and E665 [7] experimental data as well with the NNPDF collaboration [8]. Moreover, we perform a comparison of our predictions of singlet structure function obtained from nonlinear GLR-MQ equation with those obtained from linear DGLAP equation to examine the effect of nonlinear or shadowing corrections on the behaviour of singlet structure function. We further predict the logarithmic derivative of the singlet structure function and compare the results with H1 data [9, 10].

6.2 Formalism

6.2.1 General framework

The nonlinear corrections arising from the recombination of two gluon ladders into one gluon or a $q\bar{q}$ pair, modify the evolution equations of sea qurak distribution as [11]

$$\frac{\partial xq(x,Q^2)}{\partial \ln Q^2} = \frac{\partial xq(x,Q^2)}{\partial \ln Q^2}\Big|_{DGLAP} - \frac{27}{160}\frac{\alpha_S^2(Q^2)}{R^2Q^2}[xg(x,Q^2)]^2 + HT. \tag{6.1}$$

This equation is known as the GLR-MQ evolution equation for sea quark distribution. Here $q(x,Q^2)$ is the quark density and $g(x,Q^2)$ is the gluon density. The representation for the gluon distribution $G(x,Q^2) = xg(x,Q^2)$ is used. The first term on the right-hand side is given by standard linear DGLAP equation whereas the term quadratic in G is the result of gluon recombination into quarks. The negative sign in front of the non-linear term tames the strong growth of sea quark distribution generated by the linear term at very small-x and it describes the shadowing correc-

tions. HT stands for an additional term revealed by Mueller and Qiu but it is not given in all respects. Therefore this term is not taken into account in our analysis presented below. The parameter γ is calculated by Mueller and Qiu in perturbation theory and is found to be $\gamma = \frac{81}{16}$ for $N_c = 3$. The size of the nonlinear term crucially depends on the value of the correlation radius R between two interacting gluons. πR^2 is the target area occupied by the gluons. If the gluons originate from sources which occupy distinct regions in longitudinal coordinate space then R is of the order of proton radius, i.e. $R = 5$ GeV^{-1}. In that case recombination probability is very negligible [12, 13]. On the other hand, a considerable effect of recombination or shadowing corrections is expected if the gluons are condensed in hot spots [14] inside the proton, where R is considered to be of the order of the transverse size of a valence quark, i.e. $R = 2$ GeV^{-1}.

In the QCD improved parton model approximation, the structure functions are usually identified by summing quark distributions weighted by squared charges as usual

$$F_2(x, Q^2) = \sum_i e_i^2 x q_i(x, Q^2) \tag{6.2}$$

where the sum implies summation over all flavours of quarks and anti-quarks and e_i is the electric charge of a quark of type i. The F_2 structure functions measured in DIS can be written in terms of singlet and non-singlet quark distribution functions as [15]

$$F_2 = \frac{5}{18} F_2^S + \frac{3}{18} F_2^{NS} \tag{6.3}$$

As the structure function in the small-x region is mainly dominated by the gluon and sea quark distributions, therefore at small-x the non-singlet contribution can be neglected. It is reasonable to consider this from the experimental point of view as well. The H1 Collaboration presents a global fit of their data of the singlet quark distribution, $q_S = u + \bar{u} + d + \bar{d} + s + \bar{s}$, which determines practically the $F_2(x, Q^2)$ behaviour at small-x in the form $xq_S(x) = Ax^B(1-x)^C(1+Dx)$ where A, B, C and D are numerical constants at $Q^2 = 4$ GeV^2 and $x > 2 \times 10^{-4}$. At $x \leq 10^{-2}$, one can rewrite this expression as $xq_S(x) = Ax^B$ and one may neglect the non-singlet contribution within a few percent accuracy. Similarly ZEUS Collaboration presented their data for singlet quark distribution in a similar form $xq_S(x) = Ax^B(1-x)^C(1+$

$D\sqrt{x} + Ex$) with the numerical constants A, B, C, D and E at $Q^2 = 7$ GeV^2 and $x > 0.67 \times 10^{-4}$. Also in this case one can rewrite the expression in the form $xq_S(x) = Ax^B$.

Thus the contribution of the non-singlet part of the structure function can be ignored in the small-x region and in that situation Eq.(6.1) can be approximated as

$$\frac{\partial F_2^S(x,Q^2)}{\partial \ln Q^2} = \frac{5}{18}\frac{\partial F_2^S(x,Q^2)}{\partial \ln Q^2}\Big|_{DGLAP} - \frac{5}{18}\frac{27}{160}\frac{\alpha_S^2(Q^2)}{R^2Q^2}G^2(x,Q^2), \tag{6.4}$$

Again the first term of Eq.(6.4), which is the linear DGLAP equation for singlet structure function, in the leading twist approximation is given by [28]

$$\begin{aligned}\frac{\partial F_2^S(x,Q^2)}{\partial \ln Q^2}\Big|_{DGLAP} &= \frac{\alpha_s(Q^2)}{2\pi}\Bigg[\frac{2}{3}\Big(3 + 4\ln(1-x)\Big)F_2^S(x,Q^2) \\ &+ \frac{4}{3}\int_x^1 \frac{d\omega}{1-\omega}\Big\{(1+\omega^2)F_2^S\Big(\frac{x}{\omega},Q^2\Big) - 2F_2^S(x,Q^2)\Big\} \\ &+ N_F\int_x^1 \Big(\omega^2 + (1-\omega)^2\Big)G\Big(\frac{x}{\omega},Q^2\Big)d\omega\Bigg].\end{aligned} \tag{6.5}$$

6.2.2 Solution of GLR-MQ equation for singlet structure function and effects of gluon shadowing

Now to solve the GLR-MQ equation for singlet structure function we employ a Regge like behaviour of singlet structure function As discussed in chapter 5, the Regge ansatz can successfully describe the behaviour of structure functions at small-x [16]. The Regge theory is supposed to be applicable if x is small enough [17, 18] as long as Q^2 is sufficiently large that a perturbative treatment is possible. The Regge pole model gives the parametrization of the DIS structure function $F_2(x,Q^2)$ at small-x as $F_2 \propto x^{-\lambda}$ with $\lambda > 0$ [15]. To this end, we take into account a simple form of Regge like behaviour of singlet structure function as

$$F_2^S(x,Q^2) = J(Q^2)x^{-\lambda_S}, \tag{6.6}$$

where $J(Q^2)$ is a function of Q^2 and λ_S is the Regge intercepts for singlet structure function. According to Regge viewpoint, the high energy or small-x behaviour of both gluons and sea quarks are controlled by the same singularity factor in the complex angular momentum plane [16] since the same power is expected for sea quarks and gluons. Therefore likewise the value of the Regge intercept λ_G for gluon distribution function, the values of λ_S in our analysis is also taken to be 0.5 .

Again to obtain a solution of the GLR-MQ equation for singlet structure function, we have to assume a relation between singlet structure function and gluon distribution function as discussed in chapter 3 and chapter 4. The frequently used relation is [19-21]

$$G(x,Q^2) = K(x)F_2^S(x,Q^2), \tag{6.7}$$

with the ad hoc parameter $K(x)$ to be determined from phenomenological analysis.

Now employing the Regge ansatz of Eq.(6.6) for singlet structure function and using the relation defined by Eq.(6.7) in Eq.(6.4) we arrive at

$$\frac{\partial F_2^S(x,Q^2)}{\partial Q^2} = p_1(x)\frac{F_2^S(x,Q^2)}{\ln(Q^2/\Lambda^2)} - p_2(x)\frac{\left[F_2^S(x,Q^2)\right]^2}{Q^2\ln(Q^2/\Lambda^2)}, \tag{6.8}$$

The explicit forms of the functions $p_1(x)$ and $p_2(x)$ are

$$\begin{aligned} p_1(x) &= \frac{5}{9\beta_0}\Bigg[\frac{2}{3}\Big(3+4\ln(1-x)\Big) + \frac{4}{3}\int_x^1 \frac{d\omega}{1-\omega}\Big(\{(1+\omega^2)\omega^{\lambda_S} - 2\Big) \\ &\quad + N_F\int_x^1 \Big(\omega^2+(1-\omega)^2\Big)\omega^{\lambda_S}K(x)d\omega\Bigg], \end{aligned} \tag{6.9}$$

$$p_2(x) = \frac{27}{36}\frac{\pi^2\big(K(x)\big)^2}{\beta_0^2 R^2}. \tag{6.10}$$

Here we consider the leading twist approximation of the strong coupling constant $\alpha_s(Q^2) = \frac{4\pi}{\beta_0\ln(Q^2/\Lambda^2)}$ with $\beta_0 = 11-\frac{2}{3}N_f$ and N_f being the number of active quark flavours. Eq.(6.8) is a partial differential equation for the singlet structure function $F_2^S(x,Q^2)$ with respect to the variables x and Q^2. This equation can be used to examine the x-evolution of singlet structure function apart from its conventional use in Q^2-evolution. Solving of Eq.(6.8) we get

$$F_2^S(x,t) = \frac{t^{p_1(x)}}{C + p_2(x)\int t^{p_1(x)-2}e^{-t}dt}, \tag{6.11}$$

which leads us to the solution for the singlet structure function with nonlinear or shadowing corrections. Here we have use the variables $t = \ln(\frac{Q^2}{\Lambda^2})$ for convenience and C is a constant to be determined from initial boundary conditions. We note that in the kinematic region $0.6 \leq Q^2 \leq 30$ GeV^2 and $10^{-4} \leq x \leq 10^{-1}$ the solution given by Eq.(6.11) is in good agreement with the Regge ansatz of Eq.(6.6) and and satisfactorily describes the shadowing corrections to the singlet structure function.

So we restrict our analysis in this kinematic region and observe that the solution of singlet structure function with the inclusion of shadowing corrections given by Eq.(6.11) is valid in the region of small-x and moderate values of Q^2. However the solution suggested in Eq.(6.11) loose its validity at large-x and large-Q^2 where the effect of gluon recombination on the QCD evolution is very trivial.

Now we can determine the Q^2 and small-x dependence of singlet structure function from Eq.(6.11) using the appropriate boundary conditions. The physically plausible boundary conditions are

$$F_2^S(x,t) = F_2^S(x,t_0) \tag{6.12}$$

at $t = t_0$ where $t_0 = \ln\left(\frac{Q_0^2}{\Lambda^2}\right)$ for some lower value of $Q^2 = Q_0^2$ and

$$F_2^S(x,t) = F_2^S(x_0,t), \tag{6.13}$$

at some high $x = x_0$.

The boundary condition (6.12) leads us to

$$F_2^S(x,t_0) = \frac{t_0^{p_1(x)}}{C + p_2(x)\int {t_0}^{p_1(x)-2}e^{-t_0}dt_0}, \tag{6.14}$$

where $t_0 = \ln\left(\frac{Q_0^2}{\Lambda^2}\right)$. From this equation the constant C can be determined by choosing a suitable input distribution $F_2^S(x,t_0)$ at a given value of Q_0^2. Now from Eqs.(6.11) and (6.14) we get the Q^2-evolution of shadowing singlet structure function for fixed x given as

$$F_2^S(x,t) = \frac{t^{p_1(x)}F_2^S(x,t_0)}{t_0^{p_1(x)} + p_2(x)\Big[\int t^{p_1(x)-2}e^{-t}dt - \int {t_0}^{p_1(x)-2}e^{-t_0}dt_0\Big]F_2^S(x,t_0)}. \tag{6.15}$$

This expression gives the Q^2-evolution of shadowing singlet structure function at LO. We can easily compute the dependence of singlet structure function on Q^2 for a particular value of x by choosing an appropriate input distribution at a given value of Q_0^2 using Eq.(6.15). The effect of nonlinear or shadowing corrections to the singlet structure functions for a set of Q^2 can also be studied from this equation.

Similarly, the boundary condition (6.13) yields

$$F_2^S(x_0,t) = \frac{t^{p_1(x_0)}}{C + p_2(x_0)\int t^{p_1(x_0)-2}e^{-t}dt}, \tag{6.16}$$

so that using Eqs. (6.11) and (6.16) we obtain

$$F_2^S(x,t) = \frac{t^{p_1(x)} F_2^S(x_0,t)}{t^{p_1(x_0)} + \Big[p_2(x)\int t^{p_1(x)-2}e^{-t}dt - p_2(x_0)\int t^{p_1(x_0)-2}e^{-t}dt\Big] F_2^S(x_0,t)}. \quad (6.17)$$

Thus Eq.(6.17) provides us the solution of the GLR-MQ equation for singlet structure function at small-x for fixed Q^2. Using this equation the small-x dependence of nonlinear singlet structure function can be predicted for a particular value of Q^2 taking a convenient input distribution at an initial value of $x = x_0$. Eq.(6.17) further helps us to examine the effect of shadowing corrections to the singlet structure functions at small-x.

6.2.3 Comparative analysis of DGLAP and GLR-MQ equations for singlet structure function

In this section we find a solution of the linear DGLAP equation (Eq.(6.5)) for singlet structure function at LO employing the Regge ansatz of Eq.(6.6) and compare it with the solution of the GLR-MQ equation for singlet structure function discussed above. This comparison assists us to estimate the effect of shadowing corrections in our predictions of singlet structure function. Now employing the Regge ansatz of Eq.(6.6) the solution of Eq.(6.5) is obtained as

$$F_2^S(x,t) = Dt^{p_1(x)}, \quad (6.18)$$

where D is a constant to be fixed by initial boundary condition. The x dependent function $p_1(x)$ is defined in Eq.(6.9). We define

$$f_{10} = F_2^S(x,t_0) = Dt_0^{p_1(x)} \quad (6.19)$$

at $t = t_0$ at some lowe value $Q^2 = Q_0^2$. Then Eq.(6.18) and Eq.(6.19) leads us to

$$F_2^S(x,t) = f_{10}\Big(\frac{t}{t_0}\Big)^{p_1(x)}. \quad (6.20)$$

which provides the solution of the linear DGLAP equation for singlet structure function with the ansatz of Eq.(6.6) and it describes the Q^2-evolution of linear singlet structure function for a fixed value of x provided a suitable input distribution f_{10} has been chosen from the initial boundary condition.

Again, defining

$$f_{20} = F_2^S(x_0,t) = Dt^{p_1(x_0)} \quad (6.21)$$

at some initial higher value $x = x_0$, Eq.(6.18) can be expressed as

$$F_2^S(x, Q^2) = f_{20} t^{p_1(x)-p_1(x_0)}. \tag{6.22}$$

Eq.(6.22) is the solution of the linear DGLAP equation for singlet structure function at small-x with the ansatz of Eq.(6.6) and it describes the small-x behavior of linear singlet structure function for a particular value of Q^2 by choosing an appropriate input distribution f_{20} from the initial boundary condition.

Now considering the solutions of the linear DGLAP and nonlinear GLR-MQ equations respectively we can examine how the gluon recombination processes effect the linear QCD evolution of singlet structure functions. For this purpose we calculate the ratio of the solution of nonlinear GLR-MQ equation to that of linear DGLAP equation for singlet structure function using the Eqs.(6.17) and (6.22)

$$R_{F_2^S} = \frac{F_2^{S^{GLR-MQ}}(x,t)}{F_2^{S^{DGLAP}}(x,t)}, \tag{6.23}$$

as a function of variable x for different values of Q^2. From this ratio we can investigate the effect of shadowing corrections as a consequence of gluon recombination on the behavior of singlet structure function at small-x. The phenomenological analysis of Eq.(6.23) is presented in section 3.

6.2.4 Derivative of the singlet structure function with respect to $\ln Q^2$

It is very interesting to study the logarithmic derivative of the F_2 structure function with a shadowing corrections interpretation which provides information pertinent to the Regge analyses of F_2 in x and Q^2 kinematic domains. We make an attempt to study the Q^2 dependence of $\partial F_2^s/\partial \ln Q^2$ at given fixed value of x and examine the effect of shadowing corrections. There are several methods suggesting the relation between the scaling violations of $F_2(x, Q^2)$ to the gluon density at small-x [22-26]. These methods are based on the fact that at very small-x the structure function becomes gluon dominated. We use the the following approximate relation between the gluon density and the scaling violation of $F_2(x, Q^2)$ at some point x [26]

$$\frac{\partial F_2^S}{\partial \ln Q^2} = \frac{5\alpha_S(Q^2)}{9\pi} \int_x^1 \Big(\omega^2 + (1-\omega)^2\Big) G\Big(\frac{x}{\omega}, Q^2\Big) d\omega, \tag{6.24}$$

for four flavours. Since the non-singlet contributions of the structure function can be neglected in the small-x region, therefore we have considered the F_2 structure function as equivalent to F_2^S. The nonlinear gluon distribution function has a Regge like behavior

$$G(x,Q^2) = H(Q^2)x^{-\lambda_G}, \tag{6.25}$$

in the small-x region as discussed earlier in chapter 5. Thus the function $G(x/\omega, Q^2)$ can be expressed as

$$G\Big(\frac{x}{\omega}, Q^2\Big) = \omega^{\lambda_G} G(x,Q^2), \tag{6.26}$$

Using Eq.(6.24) along with the Eq.(6.26), we can express Eq.(6.4) in terms of gluon distribution function as

$$\frac{\partial F_2^S(x,Q^2)}{\partial \ln(Q^2)} = \frac{5\alpha_s(Q^2)}{9\pi} M(x) G(x,Q^2) - \frac{3\alpha_s^2(Q^2)}{64R^2Q^2} G^2(x,Q^2), \tag{6.27}$$

with,

$$M(x) = \int_x^1 \Big(\omega^2 + (1-\omega)^2\Big)\omega^{\lambda_G}. \tag{6.28}$$

Thus from Eq.(6.27) we can determine the effect of shadowing corrections on the behaviour of the logarithmic derivative of the singlet structure function. For phenomenological analysis of Eq.(6.27) we take the results of the gluon distribution function $G(x,Q^2)$ obtained in chapter 5 of this thesis. Due to the negative nonlinear term as a result of gluon recombination Eq.(6.27) is expected to predict a slower growth of $\partial F_2^s/\partial \ln Q^2$ towards small-x.

6.3 Result and discussion

We have solved the nonlinear GLR-MQ evolution equation by considering the Regge like behavior of singlet and gluon structure function and examine the effects of shadowing corrections due to gluon recombination processes at small-x to the LO DGLAP evolution equations. The behavior of singlet structure function at small-x and moderate Q^2 is investigated for both at $R = 2$ GeV^{-1} and $R = 5$ GeV^{-1} from the predicted solution of the GLR-MQ equation. Our computed values of singlet structure function with shadowing corrections are compared with the CERN's NMC [6], Fermilab E665

Collaboration [7] as well as with those obtained in the NNPDF [8] collaboration. It is worthwhile to mention here that the NMC and E665 experiments measured the deuteron structure function F_2^d from which F_2^S can be extracted using the relation $F_2^d = \frac{5}{9}F_2^S$. We perform our analysis in the kinematic region $0.6 \leq Q^2 \leq 30$ GeV^2

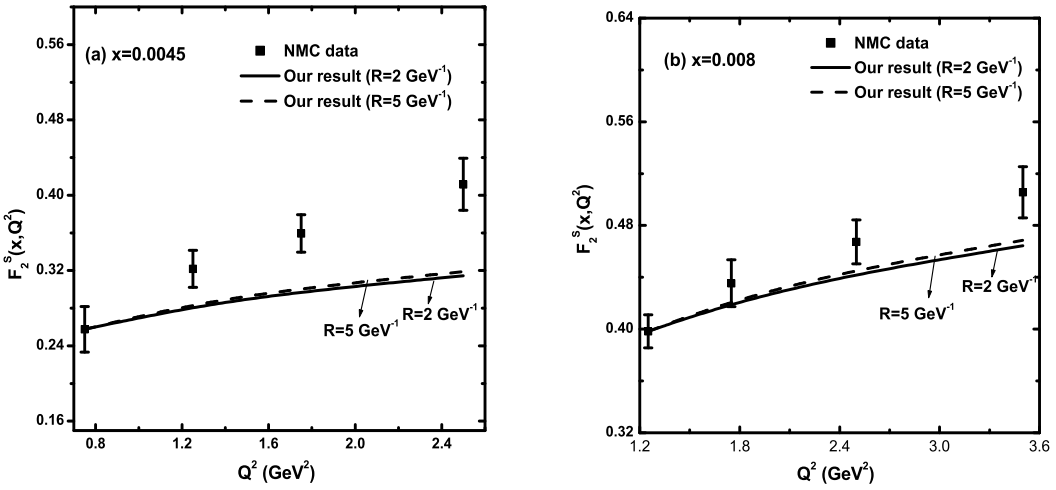

Figure 6.1: Q^2 dependence of singlet structure function with shadowing corrections for $R = 2$ GeV^{-1} (solid lines) and $R = 5$ GeV^{-1} (dash lines) computed from Eq. (6.15) compared with the NMC data [6].

and $10^{-4} \leq x \leq 10^{-1}$ where the suggested solution of the GLR-MQ equation for singlet structure function given by Eq.(6.11) is found to be legitimate. We consider the range $0.6 < Q^2 < 3.6$ GeV^2 and $10^{-4} < x < 0.013$ for NMC data, $1 < Q^2 < 4$ GeV^2 and $10^{-4} < x < 0.01$ for E665 data and $1 < Q^2 < 27$ GeV^2 and $10^{-4} < x < 0.011$ for NNPDF data in our phenomenological analysis. To compute the dependence of structure functions on Q^2 we take the input distributions from the data point corresponding to the lowest value of Q^2 for a particular range of Q^2 under study. On the other hand, the data point corresponding to the highest value of x of a particular range of x under consideration are taken as input distribution to determine the x dependence of the structure functions. In the present analysis we consider the function $K(x) = K$, where K is a constant parameter, to relate the singlet structure function and gluon densities as a simplest assumption and find that the best fit results are obtained in the range $0.28 < K < 1.2$ for our entire region of discussion. The vertical error bars represent the total combined statistical and systematic uncertainties of the experimental data.

In Figure 6.1 we plot the Q^2 dependence of singlet structure function with shad-

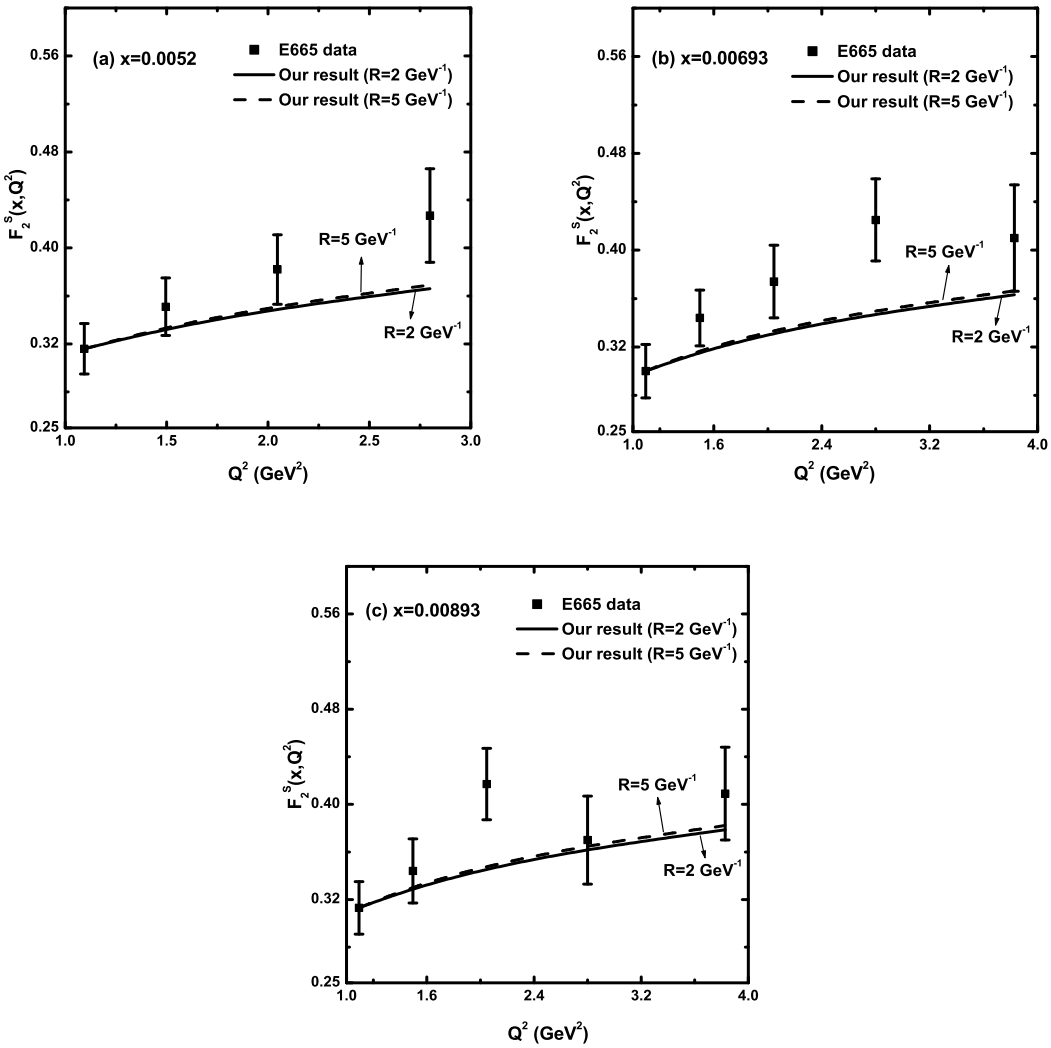

Figure 6.2: A plot showing the Q^2 dependence of singlet structure function with shadowing corrections for $R = 2$ GeV^{-1} (solid lines) and $R = 5$ GeV^{-1} (dash lines) computed from Eq. (6.15) compared with the E665 data [7].

owing corrections computed from Eq.(6.15) for $R = 2$ GeV^{-1} and $R = 5$ GeV^{-1} and check the compatibility of our predictions with the NMC data at two representative $x = 0.0045$ and 0.008 respectively. The solid lines represent the predictions of singlet structure function for the hot spots with $R = 2$ GeV^{-1} whereas the results for $R = 5$ GeV^{-1} is shown by the dash lines.

In Figure 6.2 we show the comparison of our predictions of the singlet structure function for $R = 2$ GeV^{-1} and $R = 5$ GeV^{-1} obtained from Eq.(6.15) with the E665 data. Here the predicted values of singlet structure function with shadowing corrections are plotted against Q^2 at some fixed $x = 0.0052, 0.00693$ and 0.00893 respectively. The solid lines represent the results for $R = 2$ GeV^{-1} whereas the dash

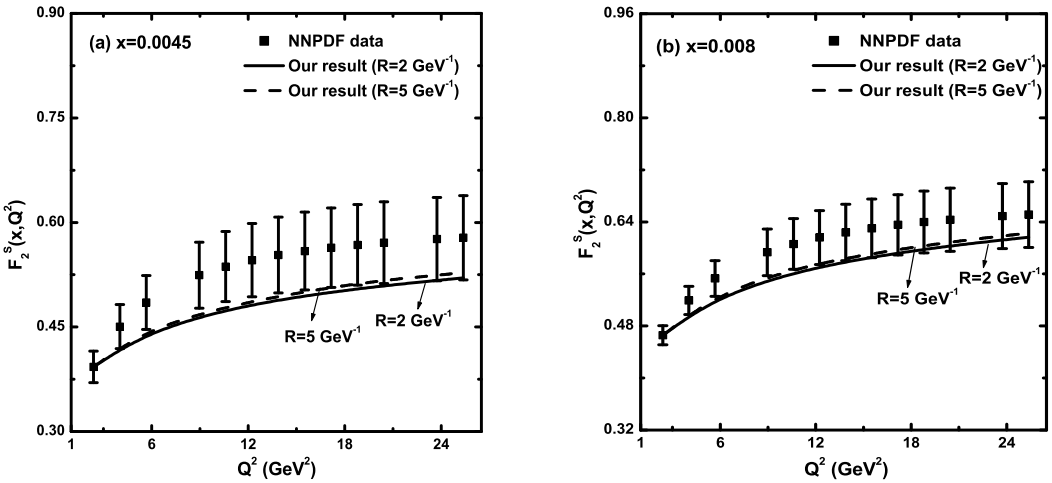

Figure 6.3: Q^2 dependence of singlet structure function with shadowing corrections for $R = 2$ GeV^{-1} (solid lines) and $R = 5$ GeV^{-1} (dash lines) obtained from Eq.(6.15) compared to NNPDF data [8].

lines represent the results for $R = 5$ GeV^{-1}.

Similarly, in Figure 6.3 the Q^2 dependence of the singlet structure function with shadowing corrections obtained from Eq.(6.15) for $R = 2$ GeV^{-1} and $R = 5$ GeV^{-1} are compared with the NNPDF parametrizations. Here the plots are shown for two values of x, viz. $x = 0.0045$ and 0.008. The results for $R = 2$ GeV^{-1} are depicted by the solid lines and the results for $R = 5$ GeV^{-1} are shown by the dash lines.

On the other hand, Figure 6.4 represents the small-x behavior of singlet structure function with shadowing corrections computed from Eq.(6.17) for $R = 2$ GeV^{-1} and $R = 5$ GeV^{-1} respectively. The consistency of our results are examined with the NMC data at fixed values of $Q^2 = 1.25, 1.75$ and 2.5 GeV^2 respectively. The results for $R = 2$ GeV^{-1} are shown by the solid lines whose those for $R = 5$ GeV^{-1} are shown by the dash lines.

In Figure 6.5 we show the comparison of the small-x behavior of singlet structure function with shadowing corrections computed from Eq.(6.17) for $R = 2$ GeV^{-1} and $R = 5$ GeV^{-1} with E665 data. The comparison is shown for four representative Q^2, viz. $Q^2 = 1.094, 1.496, 2.046$ and 2.799 GeV^2 respectively. The solid lines represent the results for $R = 2$ GeV^{-1} whereas the dash lines represent the results for $R = 5$ GeV^{-1}.

Figure 6.6 shows the plots of singlet structure function with shadowing corrections computed from Eq.(6.17) for $R = 2$ GeV^{-1} and $R = 5$ GeV^{-1} vs. x compared with

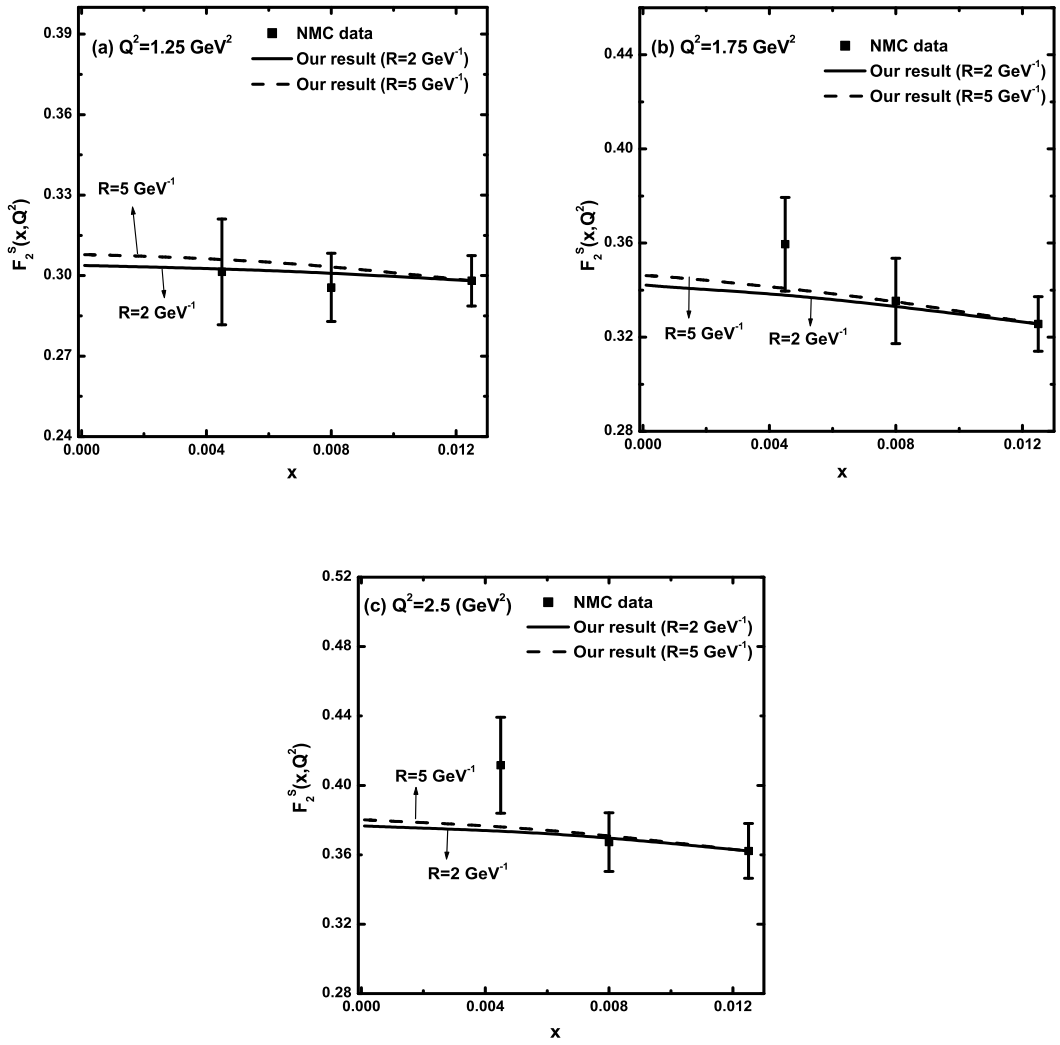

Figure 6.4: Small-x behavior of singlet structure function with shadowing corrections for $R = 2$ GeV^{-1} (solid lines) and $R = 5$ GeV^{-1} (dash lines)from Eq.(6.17) compared to NMC data [6].

the NNPDF data at four representative Q^2, viz. $Q^2 = 4.03, 8.958, 12.242$ and 18.808 GeV^2 respectively. The solid lines represent the results for $R = 2$ GeV^{-1} whereas the dash lines represent the results for $R = 5$ GeV^{-1}.

From Figure 6.1 to Figure 6.6 we observe that the obtained results of singlet structure function with shadowing corrections show the general trend of experimental data and parametrization. The singlet structure function increases with increasing Q^2 and decreasing x, but this attitude is tamed with respect to the nonlinear terms in the GLR-MQ equation. The effect of shadowing corrections as a consequence of gluon recombination processes in our predictions is observed to be very high at the hot-spot with $R = 2$ GeV^{-1} when the gluons are centered within the proton, compared to at $R = 5$ GeV^{-1} when the gluons are disseminated throughout the entire proton.

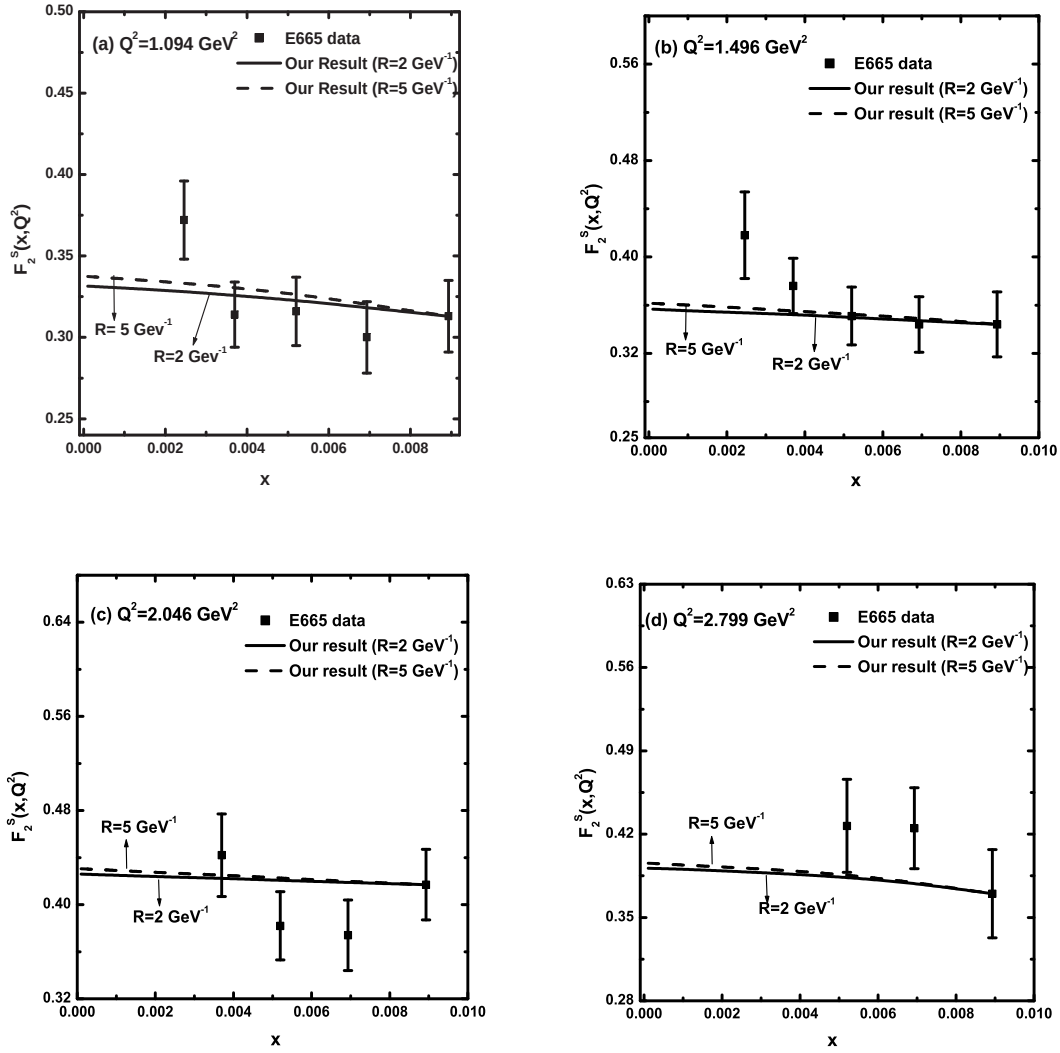

Figure 6.5: Small-x behaviour of singlet structure function with shadowing corrections for $R = 2$ GeV^{-1} (solid lines) and $R = 5$ GeV^{-1} (dash lines) computed from Eq.(6. 17) compared to E665 data [7].

Moreover, to examine the effect of nonlinear or shadowing corrections to the singlet structure function in our prediction, we plot the ratio of the solution of nonlinear GLR-MQ equation to that of the linear DGLAP equation for singlet structure function in Figure 6.7. The ratio $R_{F_2^S}$ defined in Eq.(6.22) is plotted against the variable x in the range $10^{-4} \leq x \leq 10^{-2}$ for five representative values $Q^2 = 4.03, 5.675, 8.958, 12.242$ and 18.808 GeV^2 respectively. We observe that as x grows smaller the GLR-MQ/DGLAP ratio for singlet structure function decreases which implies that the effect of nonlinearity increases towards small-x due to gluon recombination. We also observe that towards smaller values of Q^2 the value of the ratio goes smaller.

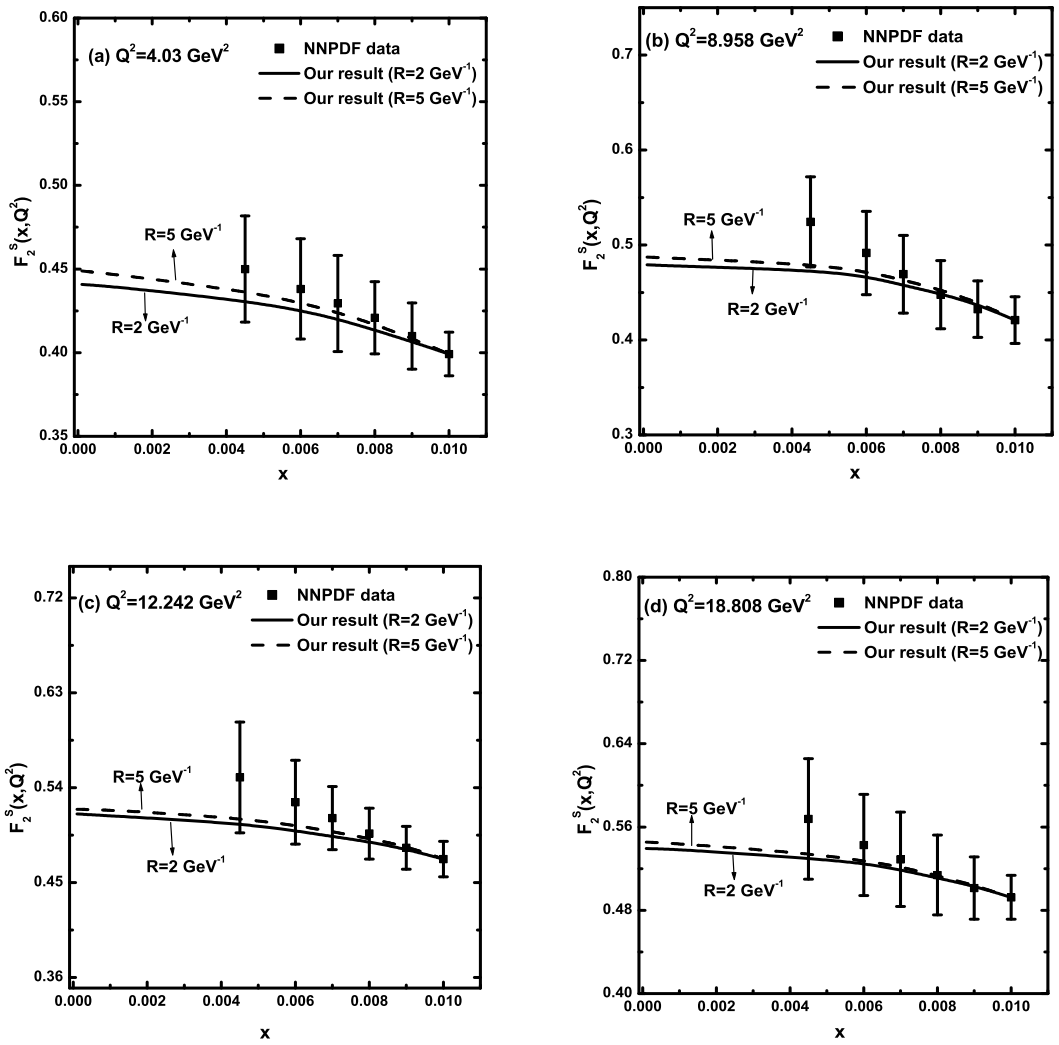

Figure 6.6: Small-x behavior of singlet structure function with shadowing corrections for $R = 2$ GeV^{-1} (solid lines) and $R = 5$ GeV^{-1} (dash lines) computed from Eq.(6.17) compared to NNPDF data [8].

In Figure 6.8 we show a plot of logarithmic derivative of the singlet structure function obtained at the hot-spot point $R = 2$ GeV^{-1} from Eq.(6.27) vs. Q^2 at three fixed values of $x = 0.0005, 0.005$ and 0.008 respectively. We compare our results with the H1 [9, 10] data. The corresponding values of $G(x, Q^2)$ are obtained from Eq.(5.15) of chapter 5 using the MRST2001LO [26] input gluon parametrization. Similarly, we show a plot of logarithmic slop of the singlet structure function for a set of x values in Figure 6.9 at two different bins in Q^2, viz. $Q^2 = 2.2$ and 7.4 GeV^2 respectively. Here also we check the consistency of our results with the H1 [9, 10] data. The corresponding values of $G(x, Q^2)$ are obtained from Eq.(5.17) of chapter 5 using the MRST2001LO [27] input gluon parametrization. We observe that the derivative of the singlet structure function with respect to $\ln Q^2$ has a tamed behavior

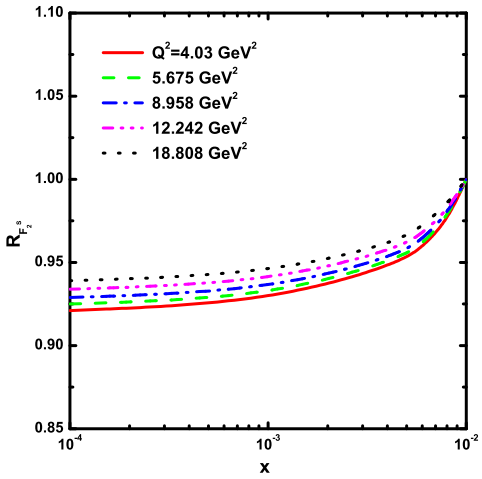

Figure 6.7: A plot of the GLR-MQ/DGLAP ratio for singlet structure function for five different bins in $Q^2 = 4.03, 5.675, 8.958, 12.242$ and 18.808 GeV^2.

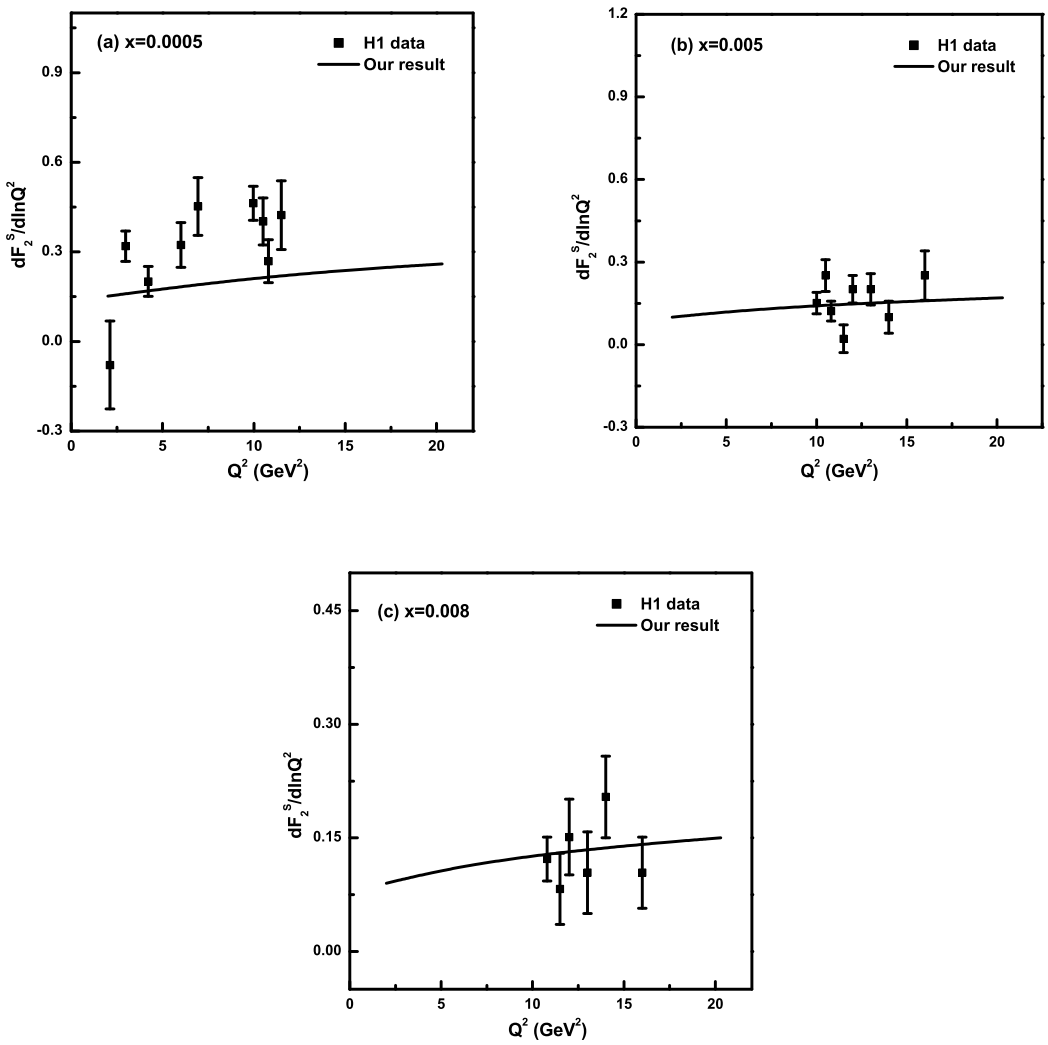

Figure 6.8: A plot of the derivative of the singlet structure function with respect to $\ln(Q^2)$ vs. Q^2 compared with the H1 data [9, 10] at $x = 0.0005, 0.005$ and 0.008 respectively.

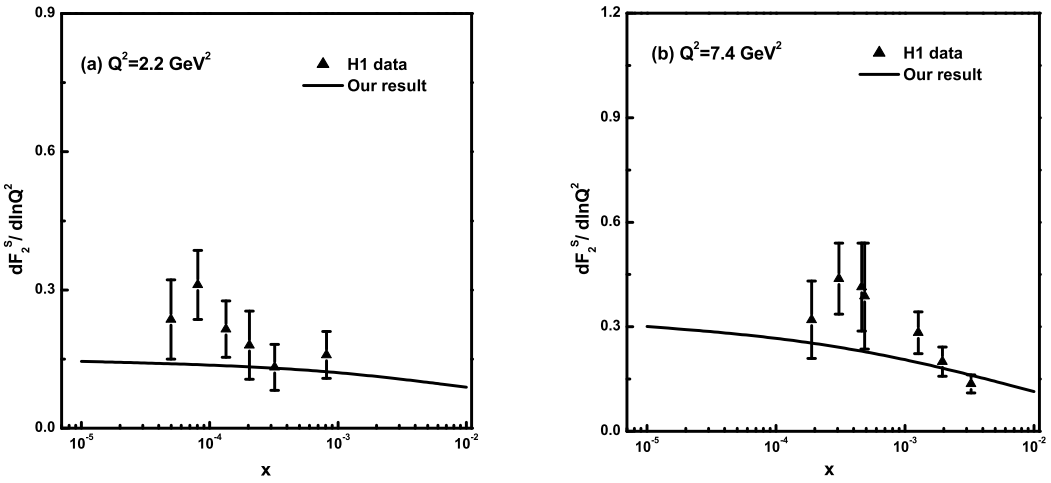

Figure 6.9: A plot of the derivative of the singlet structure function with respect to $\ln(Q^2)$ vs. x compared with the H1 data [9, 10] at $Q^2 = 2.2$ and 7.4 GeV^2.

due to gluon recombination as x grows smaller. It can be easily seen from the figure that the H1 data shows a steep rise of the logarithmic derivative of the structure function towards small-x, however this steep behavior is observed to be tamed for $x \leq 10^{-4}$. This tamed behaviour is correlated with the shadowing corrections as a result of gluon recombination at very small-x. It is very interesting to note that our results obtained in the GLR-MQ framework are comparable with the H1 data in the small-x region.

6.4 Summary

To summaries, we solve the nonlinear GLR-MQ equation for sea quark distribution function in leading twist approximation incorporating the well known Regge ansatz and investigate the effect of nonlinear or shadowing corrections arises due to the gluon recombination processes on the behavior of singlet structure function at small-x and moderate-Q^2. We note that the solution of the GLR-MQ equation for singlet structure function with shadowing corrections suggested in this work is found to be valid only in the kinematic domain $0.6 \leq Q^2 \leq 30$ GeV^2 and $10^{-4} \leq x \leq 10^{-1}$, where the gluon recombination processes play an important role on the QCD evolution. Our predictions of singlet structure function is found to show the general trend of experimental data and parametrization, nevertheless with the inclusion of the nonlinear terms, this behaviour of singlet structure function is slowed down towards small-x

leading to a restoration of the Froissart bound. Moreover the effect of shadowing corrections on the behaviour of singlet structure function with decreasing x become significant at the hot spot with $R = 2$ GeV^{-1} when the gluons and the sea quarks are assumed to condensed in a small region within the proton. The predictions of the GLR-MQ/DGLAP ratio for $F_2^S(x, Q^2)$ also indicate that the gluon recombination processes become significant towards smaller values of x and Q^2 . Moreover our results show that the behavior of the derivative of the singlet structure function with respect to $\ln Q^2$ is consistent with the H1 experimental data. Our results show that in the small-x region the logarithmic derivative of the singlet structure function has a tamed behavior related to shadowing corrections due to gluon recombination.

Bibliography

[1] Froissart, M. Asymptotic behavior and subtractions in the Mandelstam representation, *Phys. Rev.* **123**(3), 1053−−1057, 1961.

[2] Martin, A. Unitarity and high-energy behavior of scattering amplitudes, *Phys. Rev.* **129**(3), 1432−−1436, 1963.

[3] Mueller, A. H., Qiu, J. Gluon recombination and shadowing at small values of x, *Nucl. Phys. B* **268**(2), 427−−452, 1986.

[4] Gribov, L. N., Levin, E. M. and Ryskin, M. G. Semihard processes in QCD, *Phys. Rep.* **100**(1-2), 1−−150, 1983.

[5] Mueller, A. H. Small-x behavior and parton saturation: A QCD model, *Nucl. Phys. B* **335**(1), 115−−137, 1990.

[6] Arneodo, M. et al., Measurement of the proton and deuteron structure functions, F_2^p and F_2^d, and of the ratio $\sigma_L\sigma_T$, *Nucl. Phys. B* **483**(1-2), 3−−43, 1997.

[7] Adams, M. R. et al., Proton and deuteron structure functions in muon scattering at 470 GeV, *Phys. Rev. D* **54**(5), 3006−3056, 1996.

[8] Forte, S. et al., Neural network parametrization of deep inelastic structure functions, *JHEP* **2002**(JHEP05), 062, 2002.

[9] Adloff, C. et al., Measurement of neutral and charged current cross-sections in positron-proton collisions at large momentum transfer, *Eur. Phys. J. C* **13**(4), 609−−639, 2000.

[10] Adloff, C. et al., Deep-inelastic inclusive ep scattering at low x and a determination of α_s, *Eur. Phys. J. C* **21**(1), 33−−61, 2001.

[11] Prytz, K. Signals of gluon recombination in deep inelastic scattering, *Eur. Phys. J. C* **22**(2), 317−−321, 2001.

[12] Laenen, E., Levin, E. A new evolution equation, *Nucl. Phys. B* **451**(1-2), 207−−230, 1995.

[13] Laenen, E., Levin, E. Parton densities at high energy, *Annu. Rev. Nucl. Part. Sci.* **44**, 199−−246, 1994.

[14] Levin, E. M., Ryskin, M. G. Low-x structure function and saturation of the parton density, *Nucl. Phys. B (Proc. Suppl.)* **18**(3), 92−−124, 1991.

[15] Abbott, L. F., Atwood, W. B. and Michael Barnett, R. Quantum-chromodynamic analysis of eN deep-inelastic scattering data, *Phys. Rev. D* **22**(3), 582−−594, 1980.

[16] Collins, P. D., *An Introduction to Regge Theory and High-Energy Physics*, Cambridge University Press, Cambridge, 1997.

[17] Donnachie, A., Landshoff, P. V. Total cross sections, *Phys. Lett. B* **296**(1-2), 227−− 232, 1992.

[18] Donnachie, A., Landshoff, P. V. Small x: two pomerons!, *Phys. Lett. B* **437**(3-4), 408−−416, 1998.

[19] Sarma, J. K., Choudhury, D. K. and Medhi, G. K. x-distribution of deuteron structure function at low-x, *Phys.Lett. B* **403**(1-2), 139−−144, 1997.

[20] Sarma, J. K., Das, B. t evolutions of structure functions at low-x, *Phys. Lett. B* **304**(3-4), 323−−328, 1993.

[21] Baishya, R., Sarma, J. K. Method of characteristics and solution of DGLAP evolution equation in leading and next to leading order at small x, *Phys. Rev. D* **74**(10), 107702, 2006.

[22] Prytz, K. Approximate determination of the gluon density at low-x from the F_2 scaling violations, *Physics Letters B* **311**(1-4), 286−−290, 1993.

[23] Prytz, K. An approximate next-to-leading order relation between the low-x F_2 scaling violations and the gluon density, *Phys. Lett. B* **332**(3-4), 393−−397, 1994.

[24] Bora, K., Choudhury, D. K. Finding the gluon distribution of the proton at low x from F_2, *Phys. Lett. B* **354**(1-2), 151−−154, 1995.

[25] Gay Ducati, M. B., Goncalves, P. B. Analysis of low-x gluon density from the F_2 scaling violations, *Phys. Lett. B* **390**(1-4), 401−−404, 1997.

[26] Boroun, G. R. Analysis of the Logarithmic Slope of F_2 from the Regge Gluon Density Behavior at Small x, *J. of Expt. and Theor. Phys.* **111**(4), 567−−569, 2010.

[27] Martin, A. D. et al., MRST2001: partons and α_s from precise deep inelastic scattering and Tevatron jet data, *Eur. Phys. J. C* **23**(1), 73−−87, 2002.